phys. stat. sol. (b) **131**, 729 (1985)

Subject classification: 13.4 and 20.1; 6; 14.3.4; 22

Sektion Physik der Humboldt-Universität zu Berlin[1])

Electroabsorption for Deep Level to Band Transitions Accompanied by Multiphonon Processes

By

A. SCHENK, R. ENDERLEIN, and D. SUISKY

Dedicated to Prof. Dr. Dr. h. c. Dr. E. h. P. GÖRLICH on the occasion of his 80th birthday

The electroabsorption spectrum for optical transitions from a deep level to a band accompanied by multiphonon processes is calculated within the Lucovsky model. The line shape turns out to be highly sensitive to the Huang-Rhys factor and to the ratio of electrooptical and phonon energy.

Das Elektroabsorptionsspektrum für optische Übergänge aus einem tiefen Niveau in ein Band unter Beteiligung von Multiphonon-Prozessen wird im Rahmen des Lucovsky-Modells berechnet. Die Linienform hängt empfindlich vom Huang-Rhys-Faktor und vom Verhältnis der Phonon-Energie zur optoelektronischen Energie ab.

1. Introduction

Deep impurities and defects in semiconductors have attracted a growing deal of attention during the last years, mainly owing to their great importance for semiconducting devices. Theoretical developments also have contributed to the process of identifying and understanding the properties of several defects. The description of the electronic structure of deep defects and impurities without any external perturbation has been improved by theoretical self-consistent Green's function methods, but if radiative or nonradiative transitions are considered one needs in addition non-perturbative results for the wave functions to get the field- and temperature-dependent transition probabilities. Beside DLTS measurements, EPR and optical methods either with external or internal fields of p–n junctions, Schottky and surface barriers form the most powerful techniques in determining the defect nature, wave functions, binding energies, cross-sections and other properties. Thus, it is useful to study both the essential influence of a strong electric field and of multiphonon excitation and deexcitation processes on optical transitions from deep level to band states.

Compared with the plenty of publications dealing with electric field effects on interband dielectric properties the processes involving deep levels lack improved understanding because of their complexity. But it is possible to cope with the problem by adopting a three-dimensional δ-potential model which allows the exact analytical solubility even in the presence of an electric field (Vinogradov [1]). In [1] the absorption spectrum has been calculated for transitions from the impurity level to the band from which the level splits up. The same model has been applied by Enderlein et al. [2] to the case of transition from valence band to impurity states accompanied by multiphonon processes. In [2] the deep-level field effect on the multiphonon-broadened optical transition has been studied. It was found that the deep level is asymmetrically broadened and its maximum of state density is shifted. In addition density of states

[1]) Invalidenstraße 110, PSF 1297, DDR-1040 Berlin, GDR.

of the initial or final band are changed according to the Franz-Keldysh effect [3]. Which of the two mechanisms is dominating depends on the particular situation, e.g. on the binding energy of the deep level and the band effective mass. In the present paper we will follow the general approach from [2] but concentrate on the second mechanism, sometimes referred to as "half-sided Franz-Keldysh effect".

Starting with the standard multiphonon theory, the general expression for the absorption coefficient $\alpha(\omega)$ will be derived in Section 2. In Section 3 we will calculate the transition rate for impurity to band transitions on the basis of a direct two-band model using the modified Lucovsky model [1] for the deep centre. The result will be discussed for strong and low electric fields in Section 4.

2. General Expression for the Absorption Spectrum

The one-electron potential consists of the periodic lattice part $V_0(\boldsymbol{x})$, the trap potential $V_t(\boldsymbol{x})$, the diagonal part of the electron–phonon interaction $H_{ep}(\boldsymbol{x}, Q)$, the electron–photon interaction, and the potential $-e\boldsymbol{F}\cdot\boldsymbol{x}$ in an external homogeneous electric field $\boldsymbol{F}$. The decoupling procedure of the multiphonon theory is extended to our problem, where the energy spectrum is continuous due to the electric field. This requires the additional assumption that electronic transitions with transition energies comparable with an effective phonon energy can be neglected. However, in the case of deep centres a real gap will remain even for field strengths up to 10^5 V/cm and, consequently we write the total wave function $\psi_{\lambda N}$ of the coupled electron–phonon system in the usual product form $\psi_{\lambda N} = \varphi_\lambda \Phi_{\lambda N}$ with the electron states φ_λ and the lattice states $\Phi_{\lambda N}$ given by the well-known set of coupled equations in its static version,

$$\left\{-\frac{\hbar^2}{2m}\Delta + V_0(\boldsymbol{x}) + V_t(\boldsymbol{x}) - e\boldsymbol{F}\cdot\boldsymbol{x}_{\text{diag}}\right\}\varphi_\lambda = \varepsilon_\lambda^0\varphi_\lambda\,, \tag{1}$$

$$\{H_p + (\varphi_\lambda|\, H_{ep}\,|\varphi_\lambda) + \varepsilon_\lambda^0\}\,\Phi_{\lambda N} = E_{\lambda N}\Phi_{\lambda N}\,, \tag{2}$$

where H_p denotes the phonon Hamiltonian and $\boldsymbol{x}_{\text{diag}}$ the diagonal part of $\boldsymbol{x}$ with respect to the discrete component of the set of electronic quantum numbers λ, usually being the band or the deep-level index. Optical transitions from deep-level states λ into band states λ' which are assumed to be dipole allowed are calculated by applying the "Golden Rule". The result for the absorption coefficient is (cf. [4])

$$\alpha(\omega, \boldsymbol{F}) = \frac{B}{\omega}\sum_{\lambda\lambda'}\sum_{NN'} p_N\,|(\Phi_{\lambda' N'}\varphi_{\lambda'}|\ \epsilon\cdot\nabla\,|\varphi_\lambda\Phi_{\lambda N})|^2\,\delta(E_{\lambda' N'} - E_{\lambda N} - \hbar\omega) \tag{3}$$

with

$$B = \frac{4\pi^2 e^2\hbar^2}{m^2 c n V}. \tag{4}$$

In (3) ϵ denotes the polarisation vector of the radiation and p_N means the statistical weight of the lattice initial states. The λ, λ' summation extends over occupied electron initial states and empty electron final states. Owing to the static equations (1) the expression for $\alpha(\omega)$ can be written as

$$\alpha(\omega, \boldsymbol{F}) = \frac{B}{\omega}\sum_{\lambda\lambda'} |P_{\lambda'\lambda}(\boldsymbol{F})|^2\, I_{\lambda'\lambda}(\omega) \tag{5}$$

with the electronic transition matrix element

$$P_{\lambda'\lambda}(\boldsymbol{F}) = (\varphi_{\lambda'}|\ \epsilon\cdot\nabla\,|\varphi_\lambda) \tag{6}$$

and $I_{\lambda'\lambda}(\omega)$ the well-known lineshape function of the multiphonon theory [5]. If we define

$$(\varphi_\lambda|\, H_{\mathrm{ep}}\,|\varphi_\lambda) = \sum_q u_q^\lambda Q_q \tag{7}$$

and use the solutions $\Phi_{\lambda N}$ of (2), the explicit result is

$$I_{\lambda'\lambda}(\omega) = \frac{1}{2\pi\hbar}\int_{-\infty}^{\infty} \mathrm{d}\tau\, \mathrm{e}^{-i\tau\omega}\, \mathrm{e}^{\frac{i\tau}{\hbar}(\varepsilon_{\lambda'}-\varepsilon_\lambda)}\, \mathrm{e}^{\sum_q S_q g(\omega_q\tau)}\,. \tag{8}$$

Here

$$S_q = \frac{1}{2}\frac{1}{\hbar\omega_q^3}|u_q^{\lambda'} - u_q^\lambda|^2 \quad \text{and} \quad \varepsilon_\lambda = \varepsilon_\lambda^0 - \frac{1}{2}\sum_q \frac{1}{\omega_q^2}|u_q^\lambda|^2 \tag{9}$$

are, respectively, the differential Huang-Rhys factors and the electronic energies shifted by the lattice relaxation energy, and $g(\omega_q\tau)$ is given by

$$g(\omega_q\tau) = (\bar{N}_q + 1)\,\mathrm{e}^{i\omega_q\tau} + \bar{N}_q\,\mathrm{e}^{-i\omega_q\tau} - (2\bar{N}_q + 1) \tag{10}$$

($\bar{N}_q$ phonon occupation number, $\hbar\omega_q$ phonon energy).

Restricting to only one effective mode ω_0 the integral in (8) can be easily evaluated yielding [5]

$$I_{\lambda'\lambda}(\omega) = \mathrm{e}^{-S(2\bar{N}+1)}\sum_{l=-\infty}^{\infty}\left(\frac{\bar{N}+1}{\bar{N}}\right)^{l/2} \mathrm{I}_l[2S\sqrt{\bar{N}(\bar{N}+1)}]\times$$
$$\times\,\delta(l\hbar\omega_0 + \varepsilon_{\lambda'} - \varepsilon_\lambda - \hbar\omega) \tag{11}$$

(I_l modified Bessel function of the order l).

Note that according to (7) and (1) the coupling constants u_q^λ become field dependent. In the following we will neglect the electron–phonon coupling for final states. The energy difference is then given by

$$\varepsilon_{\lambda'} - \varepsilon_\lambda = \varepsilon_{\lambda'}^0 - \varepsilon_\lambda^0 + S\hbar\omega_0 \tag{12}$$

with the field-dependent Franck-Condon energy

$$\Delta_{\mathrm{FC}} = S\hbar\omega_0 = \frac{1}{2\omega_0^2}|u_0^\lambda|^2\,. \tag{13}$$

The change in $\alpha(\omega)$ is obtained by subtracting from (5) the zero field value,

$$\Delta\alpha(\omega) = \alpha(\omega, \boldsymbol{F}) - \alpha(\omega, \boldsymbol{0})\,. \tag{14}$$

3. Wave Functions and Transition Rate

The explicit calculation of electron states is carried out for a two-band model with a parabolic and isotropic valence band $E_{\mathrm{v}}(\boldsymbol{k})$ (effective mass m_{v}) and a parabolic ellipsoidal conduction band $E_{\mathrm{c}}(\boldsymbol{k})$ (effective masses m_{l}, m_{t}). We consider only direct transitions and postulate the possibility to build the deep-level states only from valence states while the continuum states are assumed to be built only from Bloch functions of the conduction band near $\boldsymbol{k} = \boldsymbol{0}$,

$$\varphi_{E\mathrm{c/t}}(\boldsymbol{x}) = \frac{1}{\sqrt{V}}\sum_{\boldsymbol{k}} A_E^{\mathrm{c/t}}(\boldsymbol{k})\,\psi_{\mathrm{c/v}\boldsymbol{k}}(\boldsymbol{x})\,. \tag{15}$$

This approach should be reasonable for deep neutral centres attached to the valence band. The set of Schrödinger equations for the two envelope wave functions reads (neglecting interband transitions and the intraband polarisation of the Bloch functions)

$$\{E_c(\boldsymbol{k}) - E + ie\boldsymbol{F}\cdot\nabla_{\boldsymbol{k}}\}\, A_E^c(\boldsymbol{k}) = 0\,, \tag{16}$$

$$\{E_v(\boldsymbol{k}) - E + ie\boldsymbol{F}\cdot\nabla_{\boldsymbol{k}}\}\, A_E^t(\boldsymbol{k}) + \sum_{\boldsymbol{k}'} (v\boldsymbol{k}|\, V_t(\boldsymbol{x})\,|v\boldsymbol{k}')\, A_E^t(\boldsymbol{k}') = 0\,. \tag{17}$$

As has been shown in [6], the exact form of the short-range potential does not affect the energy dependence of the optical cross-section for zero electric field. We take the pseudo-δ-potential

$$V_t(\boldsymbol{x}) = V_0\,\delta(\boldsymbol{x})\,[1 + \boldsymbol{x}\nabla_{\boldsymbol{x}}]\,. \tag{18}$$

It produces one bound state in the gap for zero electric field. The potential strength $V_0 = 4\pi r_0^3 E_B^0$ can be fitted to the observed zero-field binding energy E_B^0, measured from the top of the valence band (r_0 localisation radius). With the potential (18) equation (17) can be solved exactly even in the presence of an electric field [1, 2]. In one-band approximation ($E_v(\boldsymbol{k}) = -E_g - \hbar^2\boldsymbol{k}^2/2m_v$) the normalized envelope wave function $A_E^t(\boldsymbol{x})$ in $\boldsymbol{x}$ space is given by

$$A_E^t(\boldsymbol{x}) = \frac{A}{\sqrt{\mathcal{F}(\eta)}}\,\frac{1}{\sqrt{\mathcal{F}^2(\eta) + \hat{\mathcal{G}}^2(\eta)}}\int_0^\infty \mathrm{d}\varkappa\,\varkappa J_0(\varkappa\sqrt{x^2+y^2})\,\times$$

$$\times\left\{\hat{\mathcal{G}}(\eta)\,\mathrm{Ai}\,[\eta(\varkappa)]\,\mathrm{Ai}\left[\eta(\varkappa) + \frac{eFz}{\hbar\theta_v}\right] - \mathcal{F}(\eta)\,C[\eta(\varkappa); z]\right\} \tag{19}$$

with

$$A = \left[\frac{eF\hbar^2}{\pi(\hbar\theta_v)^3\,2m_v}\right]^{1/2}, \qquad \eta(\varkappa) = \frac{E - E_v(\varkappa)}{\hbar\theta_v}, \qquad \eta = \frac{E + E_g}{\hbar\theta_v}$$

and

$$\hat{\mathcal{G}}(\eta) = \frac{1}{\pi}\sqrt{\frac{E_B^0}{\hbar\theta_v}} + \mathcal{G}(\eta)\,,$$

$$C[w; z] = \theta(z)\,\mathrm{Ai}\left(w + \frac{eFz}{\hbar\theta_v}\right)\mathrm{Bi}(w) + \theta(-z)\,\mathrm{Ai}(w)\,\mathrm{Bi}\left(w + \frac{eFz}{\hbar\theta_v}\right). \tag{20}$$

The electrooptical functions $\mathcal{F}(\eta)$ and $\mathcal{G}(\eta)$ in (19) and (20) can be expressed by Airy functions in the following way:

$$\mathcal{F}(\eta) = \mathrm{Ai}'^2(\eta) - \eta\mathrm{Ai}^2(\eta)\,, \qquad \mathcal{G}(\eta) = \mathrm{Ai}'(\eta)\,\mathrm{Bi}'(\eta) - \eta\,\mathrm{Ai}(\eta)\,\mathrm{Bi}(\eta)\,, \tag{21}$$

where $\hbar\theta_v$ is the electrooptical energy,

$$\hbar\theta_v = \left[\frac{(e\hbar F)^2}{2m_v}\right]^{1/3}. \tag{22}$$

It is interesting to consider the local density of deep-centre states. Taking (19) at the origin, one obtains after simple algebra

$$\varrho_t(E) = |A_E^t(0)|^2 = (\sqrt{E_B^0\hbar\theta_v}\,4\pi^3 r_0^3)^{-1}\,\frac{\mathcal{F}(\eta)}{\mathcal{F}^2(\eta) + \hat{\mathcal{G}}^2(\eta)} \tag{23}$$

($r_0^2 = \hbar^2/2m_v E_B^0$). The spectrum (23) turns out to be an asymmetrically broadened δ-peak close to the zero-field position E_B^0 with increasing broadening for rising field strengths. The zero-field limit of (19) can be easily found using the asymptotic be-

haviour of $\mathcal{F}(\eta)$ and $\hat{\mathcal{F}}(\eta)$,

$$\lim_{F \to 0} \varrho_t(E) = (2\pi r_0^3)^{-1} \delta(E + E_g - E_B^0) . \tag{24}$$

To determine the position of the maximum of state density one has to solve the equation $\hat{\mathcal{F}}(\eta) = 0$. As long as field strengths are below a certain threshold value the asymptotic form of $\mathcal{F}(\eta)$ for large positive arguments can be applied [7],

$$\mathcal{F}(\eta) \approx -\frac{1}{\pi}\sqrt{\eta}\,(1 - 0.03123/\eta^3) , \tag{25}$$

yielding

$$E(\max\ \varrho_t) \approx E_B^0 \left[1 + 0.0625 \left(\frac{\hbar\theta_v}{E_B^0}\right)^3\right] - E_g , \tag{26}$$

where terms of higher than third order in $\hbar\theta_v/E_B^0$ have been neglected. Equation (26) expresses the quadratic Stark effect and shows that the energy shift will only be remarkable for extremely high field strengths (above 10^6 V/cm). Thus, the field effects on impurity states within the Lucovsky model are much smaller than those on band states.

To calculate the latter for a parabolic ellipsoidal conduction band we define the angle ϑ between the electric field applied in z-direction and the rotational axis of the energy ellipsoid. Then (16) has the solution

$$A^c_{Ek_{\perp 1}k_{\perp 2}}(\boldsymbol{x}) = B \exp\left[ixk_{\perp 1} + iyk_{\perp 2} - iz\beta k_{\perp 2}\right] \mathrm{Ai}\left(\frac{E_\perp - E - eFz}{\hbar\theta_{||}}\right), \tag{27}$$

where the following abbreviations have been introduced:

$$B = \frac{\sqrt{eF}}{2\pi\hbar\theta_{||}}, \quad \theta_{||}^3 = \frac{(eF)^2}{2\hbar m_{||}}, \quad E_\perp = \frac{\hbar^2 k_{\perp 1}^2}{2m_t} + \frac{\hbar^2 k_{\perp 2}^2}{2m_\perp} \tag{28}$$

and

$$\frac{1}{m_{||,\perp}} = \frac{1}{m_{t,1}} \sin^2\vartheta + \frac{1}{m_{l,t}} \cos^2\vartheta \tag{29}$$

$$\beta = \frac{m_{||}(m_l - m_t) \sin\vartheta \cos\vartheta}{m_t m_l} . \tag{30}$$

The local density of states corresponding to (23) now becomes

$$\varrho_c(E) = \int \mathrm{d}k_{\perp 1} \int \mathrm{d}k_{\perp 2}\, |A^c_{Ek_{\perp 1}k_{\perp 2}}(0)|^2 = \frac{1}{4\pi\hbar^3}\sqrt{8m_{||}m_\perp m_t}\,\sqrt{\hbar\theta_{||}}\,\mathcal{F}\left(-\frac{E}{\hbar\theta_{||}}\right). \tag{31}$$

It describes the well-known Franz-Keldysh tails below and the oscillations around the zero-field density of states above the M_0-threshold. Using (19) and (27) for the initial and final states and the relation

$$(\psi_{c\boldsymbol{k}'}| -i\hbar\nabla |\psi_{v\boldsymbol{k}}) \approx \boldsymbol{p}_{cv}(0)\, \delta_{\boldsymbol{k}\boldsymbol{k}'} \tag{32}$$

for the momentum matrix element built with Bloch functions, the field-dependent absorption coefficient can be written as

$$\alpha(\omega, \boldsymbol{F}) = B \frac{|\epsilon \cdot \boldsymbol{p}_{cv}|^2}{\hbar\omega^2} \int_{-\infty}^{\infty} \mathrm{d}E \int_{-\infty}^{\infty} \mathrm{d}E'\ D(E', E)\, I_{E'E}(\omega) , \tag{33}$$

where $D(E', E)$ denotes the transition rate for a transition $E \to E'$,

$$D(E', E) = \int_{-\infty}^{\infty} \mathrm{d}k_{\perp 1} \int_{-\infty}^{\infty} \mathrm{d}k_{\perp 2} \left| \int \mathrm{d}^3\boldsymbol{x}\, A^{c*}_{E'k_{\perp 1}k_{\perp 2}}(\boldsymbol{x})\, A^{t}_{E}(\boldsymbol{x}) \right|^2 . \tag{34}$$

By means of (19) and (27) the transition rate can be approximately performed in an analytical expression. Using the assumptions $m_v \gg m_{||}$ and $E + E_g \approx E_B^0$ it follows the simple product form

$$D(E', E) = \frac{V_0^2}{[E + E_g + (m_\perp/m_v)\, E']^2} \varrho_t(E)\, \varrho_c(E') \tag{35}$$

with the potential strength V_0, introduced in (18), and the local densities of states from (23) and (31). The denominator in (35) is known to be typical for the Lucovsky model. The E integration in (33) is due to the field effect on impurity states and includes the electron–phonon coupling constants u_0^E in the lineshape function according to (13). It can be carried out immediately by neglecting the field effect on impurity states completely. The calculation of the absorption coefficient then results in the convolution integral

$$\alpha(\omega, \boldsymbol{F}) = B \frac{|\epsilon \cdot \boldsymbol{p}_{cv}|^2}{\omega\hbar^2} 2 V_0 E_B^0 \int_{-\infty}^{\infty} \mathrm{d}E' \frac{\varrho_c(E')}{[E_B^0 + (m_\perp/m_v)\, E']^2} I(\hbar\omega - E' - E_B) \tag{36}$$

with

$$I(E) = \frac{1}{2\pi} \int_{-\infty}^{\infty} \mathrm{d}\tau \exp\left[-i\tau E + Sg(\hbar\omega_0\tau)\right], \tag{37}$$

and the assumption $m_v \gg m_{||}$ is not necessary any longer. In (36) E_B means the effective trap depth measured from the bottom of the conduction band: $E_B = E_g - E_B^0 + \Delta_{FC}$.

Equation (36) is useful for a qualitative discussion of the general lineshape of $\Delta\alpha(\omega)$ for various ratios of electrooptical and phonon energy. If we use (14), (11), (36), (38), (31) and the asymptotic form of $\mathcal{F}(\eta)$,

$$\lim_{\boldsymbol{F}\to\boldsymbol{0}} \mathcal{F}(\eta) = \frac{1}{\pi}\theta(-\eta)\sqrt{-\eta}\,, \tag{38}$$

the field-induced change in $\alpha(\omega)$ finally can be expressed as a sum of thermally weighted electrooptical functions of the first kind,

$$F(\eta) = \pi\mathcal{F}(\eta) - \theta(-\eta)\sqrt{-\eta}\,, \tag{39}$$

$$\Delta\alpha(\omega) = \alpha_0\, \mathrm{e}^{-S(2\bar{N}+1)} \sum_{l=-\infty}^{\infty} \left(\frac{\bar{N}+1}{\bar{N}}\right)^{l/2} \mathrm{I}_l[2S\sqrt{\bar{N}(\bar{N}+1)}] \times$$

$$\times \frac{\sqrt{\hbar\theta_{||}}\, F[(E_B + l\hbar\omega_0 - \hbar\omega)\, (\hbar\theta_{||})^{-1}]}{\omega[E_B^0 - (m_\perp/m_v)\, (E_B + l\hbar\omega_0 - \hbar\omega)]^2}. \tag{40}$$

In Fig. 1 we have plotted lineshapes at $T = 10$ K for various field strengths and Huang-Rhys factors using (40). The zero-phonon line exhibits a pure shape of the electrooptical function F, slightly modified by the energy denominator in (40). For high fields the lineshape is determined by F, which gets increasingly broadened with rising coupling strengths and the first zero value of which turns out to be shifted by the Franck-Condon energy Δ_{FC} (Fig. 1a). The discrete nature of the spectrum due to

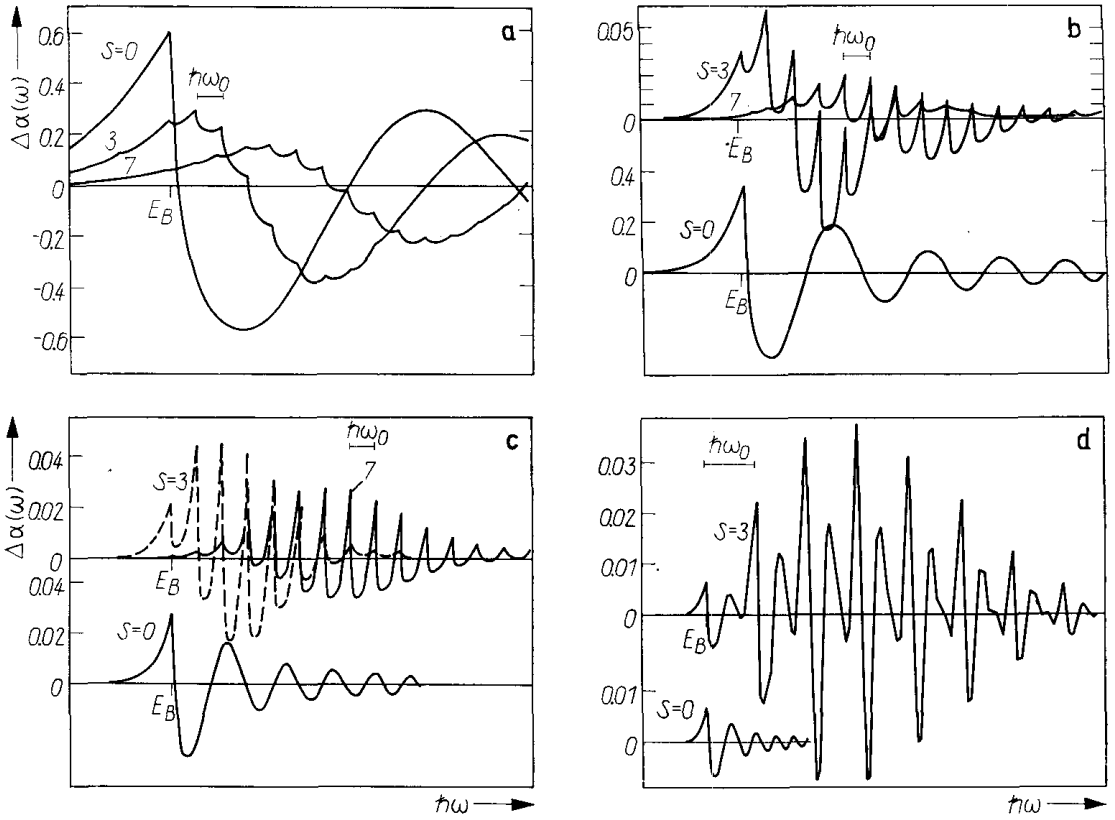

Fig. 1. Electroabsorption spectrum $\Delta\alpha(\omega)$ for different Huang-Rhys factors $S = 0$, $S = 3$, $S = 7$. The following parameters have been used: a) $\hbar\theta_{||} = 113$, b) 39, c) 24, and d) 5 meV. (Here the curve for $S = 7$ has been omitted for clarity.) $\hbar\omega_0 = 20$ meV, $E_B/\hbar\omega_0 = 30$, $T = 10$ K. The energy scale is in units of the effective phonon energy $\hbar\omega_0$. E_B denotes the trap depth

the Einstein model, which is only weak for large field strengths, becomes dominant in the case of lower fields. Below a certain electrooptical energy, when the first oscillation of F has an energetic distance less than the effective phonon energy, additional substructures arise (Fig. 1d). The height of the peaks can grow with decreasing fields now, depending on whether a maximum of $F(\eta)$ (39) coincides with $\hbar\omega_0$ or not. Mironov et al. [8] who have measured the electroabsorption spectrum of a Cr level to conduction band transition report the same effect.

4. Strong- and Low-Field Limits

According to (36) the field-induced change in $\alpha(\omega)$ is given by the convolution integral

$$\Delta\alpha(\omega) = \frac{C\sqrt{\hbar\theta_{||}}}{\omega} \int_{-\infty}^{\infty} \mathrm{d}E' \frac{F\left(\frac{E'}{\hbar\theta_{||}}\right)}{[E_B^0 - (m_\perp/m_v)\, E']^2}\, I(\hbar\omega - E_B + E')$$

$$C \equiv \frac{\alpha_0 \sqrt{8 m_{||} m_\perp m_t}}{4\pi^2\hbar^3}. \tag{41}$$

4.1 Strong fields

For strong electric fields the general lineshape is determined by the electrooptical function. To see this we write (41) as

$$\Delta\alpha(\omega) = \frac{C\sqrt{\hbar\theta_{||}}}{\omega} \int_{-\infty}^{\infty} \mathrm{d}E' \, \frac{F(E')}{[E_B^0 - (m_\perp/m_v)\,\hbar\theta_{||}E']^2} \times$$
$$\times \frac{1}{2\pi} \int_{-\infty}^{\infty} \mathrm{d}\tau \, \mathrm{e}^{-i\tau\left[\frac{\omega}{\theta_{||}} - \frac{E_B}{\hbar\theta_{||}} + E'\right]} \, \mathrm{e}^{Sg\left(\frac{\omega_0}{\theta_{||}}\tau\right)}. \tag{42}$$

We expand $g\left(\frac{\omega_0}{\theta_{||}}\tau\right)$ to second order in the phase factors,

$$g\left(\frac{\omega_0}{\theta_{||}}\tau\right) \approx i\tau\frac{\omega_0}{\theta_{||}} - \frac{\tau^2}{2S}\frac{\Gamma^2}{\theta_{||}^2}, \tag{43}$$

with the attenuation constant $\Gamma = \omega_0\sqrt{S(2\bar{N}+1)}$. This is justified if the condition $\omega_0/\theta_{||} \ll 2\bar{N}+1$ holds. The linear term of (43) yields the Franck-Condon shift of the zero-phonon expression,

$$\Delta\alpha^{(1)}(\omega) = \frac{C\sqrt{\hbar\theta_{||}}}{\omega} \frac{F\left(\frac{E_B + \Delta_{FC} - \hbar\omega}{\hbar\theta_{||}}\right)}{[E_B^0 + (m_\perp/m_v)(\hbar\omega - E_B - \Delta_{FC})]^2}. \tag{44}$$

If the second-order term is taken into account, a Gaussian broadening of $\Delta\alpha^{(1)}(\omega)$ occurs,

$$\Delta\alpha^{(2)}(\omega) = \frac{\hbar}{\sqrt{2\pi}\,\Gamma} \int_{-\infty}^{\infty} \mathrm{d}\omega' \, \Delta\alpha^{(1)}(\omega - \omega') \, \mathrm{e}^{-\omega'^2/2\Gamma^2}. \tag{45}$$

The resulting lineshape is then given by a shifted and damped electrooptical function F. Expression (45) cannot be evaluated in closed form. Numerical results for 400 K in comparison with those from (40) are given in Fig. 2.

Due to the Gaussian broadening only the general form of the spectrum is preserved, phonon replicas do not occur. This corresponds to the experimental situation of high temperatures.

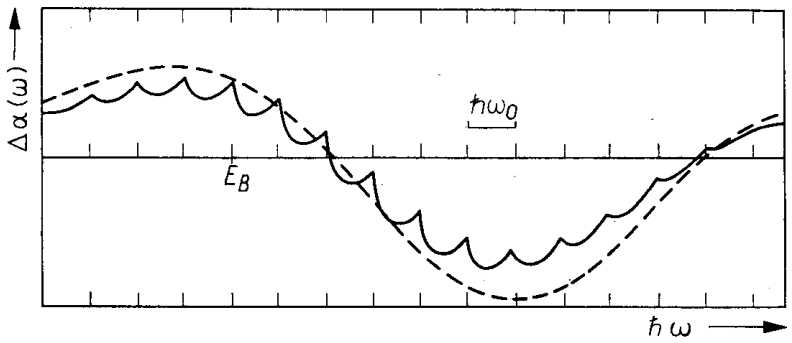

Fig. 2. Comparison of strong-field spectrum (dashed line) with the general form derived from (40). The following parameters have been used: $\hbar\theta_{||} = 113$ meV, $\hbar\omega_0 = 20$ meV, $S = 3$, $T = 400$ K

4.2 Low fields

For sufficiently low electric fields, $\Delta\alpha(\omega)$ can be approximated by the first non-vanishing term of a power series with respect to the field strength. Therefore, we write (41) in the form

$$\Delta\alpha(\omega) = \frac{C}{\omega} \int_{-\infty}^{\infty} \mathrm{d}\omega' \left\{ \frac{\left(\mathrm{Ai}\,\dfrac{\omega' - \omega}{\Omega_{||}}\right)}{\Omega_{||}} - \delta(\omega' - \omega) \right\} \times$$

$$\times \int_{-\infty}^{\infty} \mathrm{d}E'\, \theta(E')\, \sqrt{E'}\, \frac{I(\hbar\omega' - E' - E_B)}{[E_B^0 + (m_\perp/m_v)\,(E' - [\hbar\omega' - \hbar\omega])]^2} \tag{46}$$

with $\Omega_{||} = \theta_{||}/2^{2/3}$ and neglect the $(\omega' - \omega)$-dependence of the energy denominator, since $\mathrm{Ai}\left(\dfrac{\omega' - \omega}{\Omega_{||}}\right)$ is localised at $\omega = \omega'$ for low fields. This enables us to express $\alpha(\omega, \boldsymbol{F})$ by convoluting the zero-field value with $\mathrm{Ai}\left(\dfrac{\omega' - \omega}{\Omega_{||}}\right)$,

$$\alpha(\omega, \boldsymbol{F}) = \frac{1}{\omega} \int_{-\infty}^{\infty} \mathrm{d}\omega'\, \omega' \frac{\mathrm{Ai}\left(\dfrac{\omega' - \omega}{\Omega_{||}}\right)}{\Omega_{||}} \alpha(\omega', \boldsymbol{0})\,. \tag{47}$$

We expand $\mathrm{Ai}\left(\dfrac{\omega' - \omega}{\beta}\right)\Big/\beta$ to second order in $\boldsymbol{F}$,

$$\frac{\mathrm{Ai}\left(\dfrac{\omega' - \omega}{\beta}\right)}{\beta} \approx \delta(\omega' - \omega) + \frac{\beta^3}{3} \frac{\mathrm{d}^3}{\mathrm{d}\omega^3} \delta(\omega' - \omega) \tag{48}$$

to obtain

$$\Delta\alpha(\omega) \approx \frac{\Omega_{||}^3}{3\omega} \frac{\mathrm{d}^3}{\mathrm{d}\omega^3} [\omega\alpha(\omega, \boldsymbol{0})]\,. \tag{49}$$

The effective expansion parameter β of (48) can be found from (46) and (45) to be the ratio of $\Omega_{||}$ and $\sqrt{2}\,\Gamma$. Therefore, (49) is expected to be a good approximation, if the characteristic electrooptical frequency $\Omega_{||}$ is small compared with the multiphonon broadening frequency Γ, i.e.

$$\frac{\Omega_{||}}{\omega_0} \ll \sqrt{2S(2\bar{N} + 1)}\,.$$

Expressions (47) and (49) are identical with those derived by Aspnes et al. [4] for the case of optical interband transitions in the low-field limit. There $\hbar\Omega$ must be small compared to the lifetime broadening $\hbar\gamma$ of the transition. In our case the relevant energy of the unperturbed system is the multiphonon broadening energy $\hbar\Gamma$. The use of the third-derivative expression (49) involves the problem of strong divergences at energies $E_B + n\hbar\omega_0$ owing to the Einstein model. However, in reality additional lifetime broadening processes due to phonon–phonon interaction and electronic scattering mechanisms are present giving rise to additional Lorentzian broadening of the spectrum. On the other hand, at high temperatures (large Γ) phonon dispersion and other phonon branches smooth out the multiphonon substructure, which is a consequence of adopt-

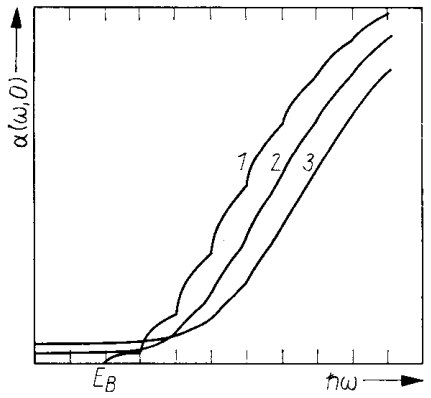

Fig. 3. Zero-field spectrum for various Lorentzian broadening parameters: (1) $\gamma = 0$, (2) 0.005, and (3) 0.01. The curves are shifted by $\hbar\omega_0$ for clarity. Parameters: $S = 3$, $E_B/\hbar\omega_0 = 30$, $T = 10$ K

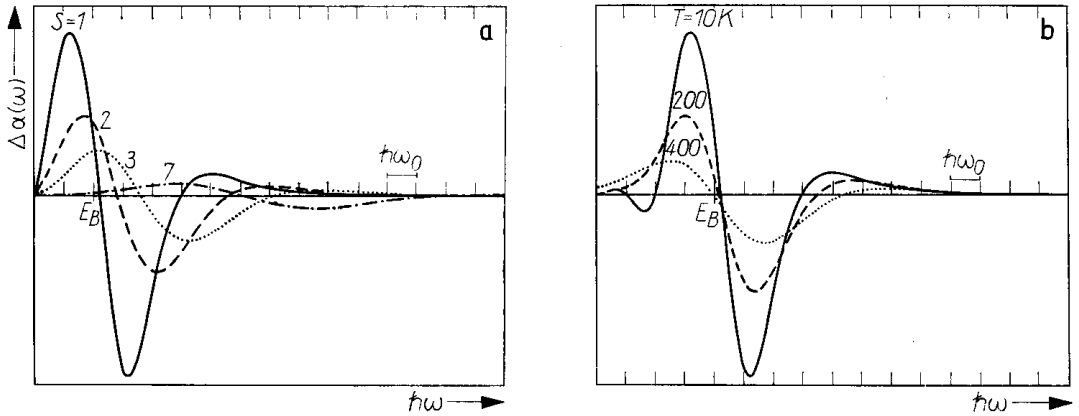

Fig. 4. Low-field spectrum without Lorentzian broadening for a) various electron–phonon coupling strengths ($E_B/\hbar\omega_0 = 30$, $T = 10$ K); b) different temperatures ($E_B/\hbar\omega_0 = 30$, $S = 1$)

ing only one phonon-mode. To illustrate both effects we have plotted the zero-field absorption spectrum for various Lorentzian broadening parameters γ in Fig. 3. Regarding the case when the multiphonon fine structure is smoothed out completely, the envelope curve of $\alpha(\omega,\boldsymbol{0})$ has been utilized to calculate $\Delta\alpha(\omega)$ by means of the third derivative of the former according to (49). The result is the well-known third-derivative lineshape of a damped square-root threshold. Numerical results for various values of S and T are given in Fig. 4. The curves show two characteristic features: The minimum

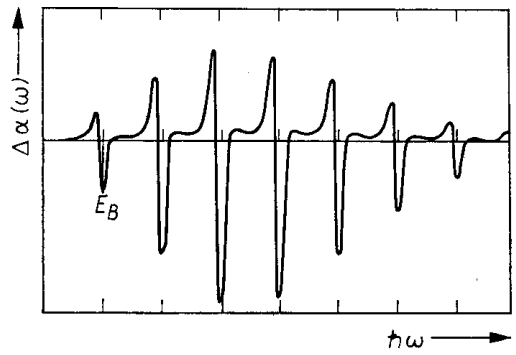

Fig. 5. Low-field spectrum after (49) with Lorentzian broadening, $\gamma = 0.04$. Parameters: $E_B/\hbar\omega_0 = 30$, $T = 10$ K, $S = 1$)

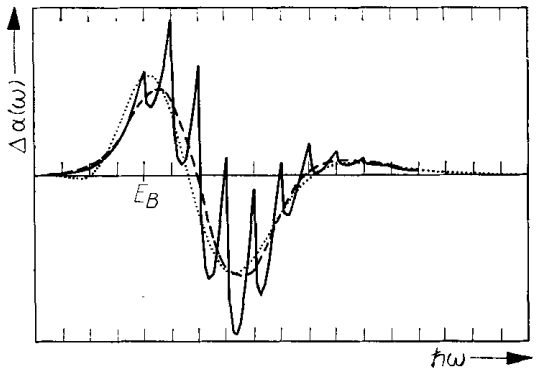

Fig. 6. Comparison of low-field spectrum (dotted line) and averaged spectrum after (40) (dashed line). The following parameters have been used: $\hbar\theta_{||} = 39$ meV, $\hbar\omega_0 = 20$ meV, $T = 10$ K, $S = 3$, $\sqrt{2}\,\Gamma/\theta_{||} = 1.3$

turns out to be localised very close to $E_B + \Delta_{FC}$ and the halfwidth of the negative peak is about $\sqrt{2}\,\hbar\Gamma = \sqrt{2S}\,\hbar\omega_0\sqrt{2\bar{N}+1}$.

If a Lorentzian broadened multiphonon fine structure is taken into account, the low-field spectrum (49) is in general agreement with that calculated from (40) (cf. Fig. 1 d). A typical lineshape for this case is shown in Fig. 5. The absence of secondary oscillations is a consequence of the low-field limit.

Fig. 6 exhibits a direct comparison of low-field approximation with smooth zero-field spectrum and lineshape calculated from (40). The dashed line indicates the averaged spectrum of (40) obtained by an average procedure over the energetic distance $\hbar\omega_0$. These lineshape are expected, if phonon dispersion and other phonon branches smooth out the multiphonon substructure due to the Einstein model. A comparison with the low-field lineshape shows the latter to be a good approximation for $\sqrt{2}\,\Gamma/\Omega_{||} \geqq 3$.

References

[1] V. C. Vinogradov, Fiz. tverd. Tela **13**, 3266 (1971).
[2] R. Enderlein, D. Fiddicke, F. Bechstedt, K. Peuker, and R. S. Bauer, Luminescence Conf., Berlin (West) 1981.
[3] W. Franz, Z. Naturf. **13a**, 484 (1958).
L. V. Keldysh, Zh. eksper. teor. Fiz. **34**, 1138 (1958).
[4] D. E. Aspnes, P. Handler, and D. F. Blossey, Phys. Rev. **166**, 921 (1968).
[5] K. Huang and A. Rhys, Proc. Roy. Soc. **A204**, 406 (1950).
[6] G. Lucovsky, Solid State Commun. **3**, 299 (1965).
[7] D. E. Aspnes, Phys. Rev. **153**, 972 (1967).
[8] A. G. Mironov, V. A. Morozova, and V. S. Vavilov, phys. stat. sol. (b) **127**, 359 (1985).

(Received August 7, 1985)

Note added in proof

Experimental electroabsorption spectra have been reported by Sokolov et al. (V. I. Sokolov, A. E. Nikoforov, V. V. Chernyaev, and S. Yu. Shashkin, Zh. eksper. teor. Fiz., Pisma **33**, 189 (1981)) for ZnSe:Ni^{2+} in the energy range between 2.64 and 2.75 eV.

The lineshape can be interpreted in terms of the low field case ($F = 2 \times 10^4$ Vcm^{-1}) where the characteristic Franz-Keldysh oscillations in the energy range between the phonon satellites should appear (see Fig. 1 d). In this case the amplitude of the positive and negative scillations is determined by the phononic part of the lineshape function ((see (37) and Fig. 1 d).